Influence of concrete strength on crack development in SFRC members

Giuseppe Tiberti [a], Fausto Minelli [a,*], Giovanni A. Plizzari [a], Frank J. Vecchio [b]

[a] DICATAM – Department of Civil Engineering, Architecture, Environment, Land Planning and Mathematics, University of Brescia, Italy
[b] FACI, Department of Structural Engineering, University of Toronto, Canada

ARTICLE INFO

ABSTRACT

Tension stiffening is still a matter of discussion into the scientific community; the study of this phenomenon is even more relevant in structural members where the total reinforcement consists of a proper combination of traditional rebars and steel fibers. In fact, fiber reinforced concrete is now a worldwide-used material characterized by an enhanced behavior at ultimate limit states as well as at serviceability limit states, thanks to its ability in providing a better crack control.

This paper aims at investigating tension stiffening by discussing pure-tension tests on reinforced concrete prisms having different sizes, reinforcement ratios, amount of steel fibers and concrete strength. The latter two parameters are deeply studied in order to determine the influence of fibers on crack patterns as well as the significant effect of the concrete strength; both parameters determine narrower cracks characterized by a smaller crack width.

© 2013 Elsevier Ltd. All rights reserved.

1. Introduction

The use of Fiber Reinforced Concrete (FRC) and especially Steel Fiber Reinforced Concrete (SFRC) has gained considerable attention in recent years, as demonstrated by its recent inclusion in the *fib* Model Code 2010 [1] and by many international committees [2] and conferences devoted to FRC [3–5].

FRC has been particularly used in several structural elements when crack propagation control is of primary importance [6], such as in precast tunnel segments [7] or in beams where little or no shear reinforcement is provided [8,9]. In several of these structural applications, the total amount of reinforcement generally consists of a combination of conventional rebars and fibers.

If the addition of fibers in a classical beam, having longitudinal reinforcement, does not necessarily provide benefits in term of load capacity and, especially, ductility at ultimate limits states (ULS) [10], there is a general consensus on the significant advantages in term of behavior at serviceability limit states (SLS), i.e. crack and deflection control.

In service conditions, the deformation of a rebar embedded in concrete is significantly influenced by the bond between the two materials. In fact, after cracking, bond transfers tensile stresses from the rebar to the surrounding concrete (between cracks), which stiffens the response of a RC member subjected to tension; this stiffening effect is referred to as "tension stiffening". Several authors already studied this mechanism in traditional RC elements [11–13], generally made of Normal Strength Concrete (NSC). In fibrous RC elements, the bridging effect of the fibers provides an additional significant mechanism that influences the transmission of tensile stresses across cracks. The combination of these two mechanisms (tension stiffening and the post-cracking residual strength provided by fibers at any crack, referred to as "residual strength" in the following) results in a different crack pattern, characterized by a reduced crack spacing and crack width. In addition, the collapse mode and the ductility of FRC elements may also be affected by stress concentrations due to enhanced bond and the residual tensile stress at a crack [10].

A number of research studies have been carried out so far on the tensile behavior of SFRC members: Mitchell and Abrishami [14] presented one of the first studies by clarifying the beneficial effect of fibers in determining narrower and closely spaced cracks, as well as in mitigating the splitting cracks in the end regions while having low concrete covers. Fields and Bischoff [15] and Bischoff [16] performed monotonic and cyclic tension-stiffening tests and included shrinkage effects in the analysis. Noghabai [17] proposed an analytical model which describes the behavior of tie-elements based on the observation of experimental tests. Analytical models were also proposed for the prediction of the behavior of FRC tension members [18–20].

* Corresponding author. Address: DICATAM – Department of Civil Engineering, Architecture, Environment, Land Planning and Mathematics, University of Brescia, Via Branze, 43, 25123 Brescia, Italy. Tel.: +39 030 3711 223; fax: +39 030 3711 312.
E-mail address: fausto.minelli@ing.unibs.it (F. Minelli).
URL: http://dicata.ing.unibs.it/minelli/ (F. Minelli).

However, none of these studies were broad enough to clearly identify the influence of fibers regarding their content, materials, combination, volume fraction and aspect ratios, all factors influencing the toughness of the composite (FRC). Moreover, none of these studies have been comprehensive in terms of the number of specimens tested or in the parameters considered.

In addition, the crack spacing is also rather influenced by the concrete strength, even though most of the analytical models published for predicting the crack spacing do not consider this effect, being on the conservative side in design.

This clearly underlines that further research has to be done in order to better understand the cracking mechanism in FRC, having either normal or high strength. Concerning the latter point, a number of authors already investigated the steel-to-concrete bond in concretes with different strengths: Reza Esfahani and Rangan [21] carried out several tests on short length pull-out specimens using NSC and HSC. By combining their results with those of other researchers, they proposed a relationship between the cracking bond strength normalized to the tensile strength of concrete, τ_{bm}/f_{ctm}, as a function of the compressive strength. Significant higher values of τ_{bm}/f_{ctm} in specimens with greater concrete strength were found: this higher ratio leads to a reduction of the transfer length necessary to restore the tensile strength into the concrete, which determines a crack spacing decrease.

The crack spacing formulation proposed in MC2010 [1] does not explicitly include this tendency, since the τ_{bm}/f_{ctm} ratio is assumed to be constant (1.8 for instantaneous loading).

The present paper describes a number of experimental results from a collaborative research program developed by the University of Brescia (Italy) and the University of Toronto (Canada), aimed at studying crack formation and development in SFRC structures made of different concrete grades. A set of tension stiffening tests was carried out by varying the concrete strength, the reinforcement ratio, the fiber volume fraction and the fiber geometry. Brescia tested and interpreted tension members made of NSC while Toronto tested identical members made of HSC, with a concrete strength of around 60 MPa and higher. A total of 59 uni-axial tension HSC specimens were tested at the University of Toronto (Canada), in addition to several material tests to quantify the concrete properties; complete details of the experimental program and the full experimental results are provided by Deluce and Vecchio [22]. A total of 109 tests were done at the University of Brescia on NSC; details of this experimentation are reported in [23] and in [24], respectively.

After a brief recall of the experiments, focus on the effect of concrete strength and fibers on the behavior exhibited by the specimens, in terms of crack formation and development, will be presented and discussed. The results will be also compared against the formulations proposed by CEB Model Code 1978 [25] and *fib* Model Code 2010 [1]; the latter also includes a section concerning FRC structures.

Finally, the ample experimental results of this investigation could be used to develop improved formulations for crack spacing, crack width and tension stiffening behavior in SFRC.

2. Experimental investigation

The experimental program was designed so that a comprehensive database of uni-axial tension tests of reinforced concrete RC and SFRC members containing a central steel rebar could be generated. These fibrous and non-fibrous members will be identified as RC and SFRC tensile ties, respectively. NSC/HSC will be used to underline the different concrete strength. Therefore, HSFRC will indicate a HSC member containing fibers whereas HSRC the corresponding non-fibrous sample (the same notation is adopted for NSRC and NSFRC specimens).

The following key-parameters were investigated:

– Concrete cylinder compressive strength from 25 MPa to 95 MPa.
– Element size: square prism having side from 50 to 200 mm.
– Clear concrete cover: from 20 to 85 mm.
– Effective reinforcing ratio, ρ_{eff}: from 0.98% to 4.17%.
– Rebar diameter $\varnothing$: from 10 to 30 mm.
– $\varnothing/\rho_{eff}$ ratio: from 271 mm to 2043 mm.
– Specimen length: from 950 mm to 1500 mm.
– Volume fraction of fibers V_f: from 0% to 1.5%.

Note that the effective reinforcement ratio (ρ_{eff}) is the reinforcing area over the area of concrete in tension surrounding the reinforcement: in these samples, $\rho = \rho_{eff}$.
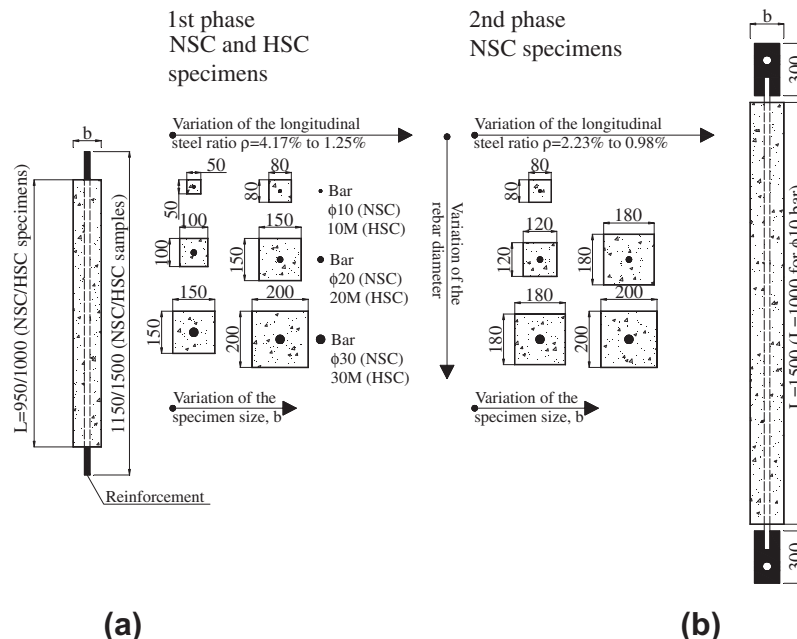

Fig. 1. Geometry and reinforcement details of specimens (1st (a) and 2nd (b) phase).

2.1. RC and SFRC uni-axial tension test specimen configurations

In a first phase of the experimental research, 64 prismatic NSC tensile members containing conventional steel reinforcing rebars having the geometry shown in Fig. 1a were cast at the University of Brescia. Each specimen was 950 mm long and five square cross sections were selected (50, 80, 100, 150 and 200 mm size). Reinforcing bars having a diameter of 10, 20 and 30 mm (B450C steel, according to European standard EN 10080, [26]), corresponding to a reinforcement ratio (ρ) varying from 1.25% to 3.26%, were used. At the University of Toronto, 59 HSC members, having the same cross-sections and a length equal to 1000 mm, were cast and tested. The deformed steel reinforcing bar sizes varied from 10M to 30M (Canadian bar sizes, [27]). Consequently, for HSC tensile ties the reinforcement ratio (ρ) ranging from 1.35% to 4.17%. The properties of the reinforcing bars used in NSC and HSC tie elements are reported in Table 1.

A second phase of research was developed only at the University of Brescia in order to better investigate the behavior of NSC tensile members. With this purpose, a further 45 prismatic ties were cast and tested; reinforcing bars having the same diameter were used, whereas four square cross sections were selected (80, 120, 180 and 200 mm size) and a reinforcement ratio ρ ranging from 0.98% to 2.23% was adopted. The specimens having a rebar diameter equal to 20 and 30 mm were longer with respect to those of the previous phase (1500 mm vs. 950 mm), with the aim of better evaluating the crack spacing (the number of expected cracks is higher with increasing length). Members with a rebar diameter equal to 10 mm were 1000 mm long. The geometry and reinforcement details of specimens belonging to the second phase are depicted in Fig. 1b.

Different dosages and types of steel fibers were included in the NSC matrix: both macroand microfibers were adopted with a total volume fraction up to 1.0%. The microfibers were only used in addition to macrofibers in formulating a hybrid system that could help both with regard to early cracking (controlled by microfibers) and for diffused macro-cracking (mainly controlled by macrofibers).

In regards to the HSC elements, three types of macrosteel fibers (hooked-end) were used, in varied volumetric contents with a total dosage up to 1.5%.

Based on the different combinations of concrete strength and fibrous reinforcement, a total of 14 test series were tested, as summarized in Table 2. Regarding the HSC elements (first phase), the experimental program included one non-fibrous RC control series and five series containing steel fibers. For the NSC elements, two RC and six SFRC series were globally tested (first and second phase). For each series, Table 2 reports the material series identification (batch ID), the volume fraction of steel fibers used and fiber designations. Note that the designations used for each fiber type denotes the fiber length as the first number and the fiber diameter as the second. Table 3 summarizes the main characteristics of all five fiber typologies.

Each combination of fiber reinforcement, member dimension and steel reinforcement ratio defines a specific set of tests, whose repetitions and notations are listed in Table 4.

2.2. Material properties

A number of material tests were conducted in order to determine the material properties of the concretes used in the RC and SFRC tensile ties. Regarding the NSC series, standard tests on 150 mm cubes were carried out. The tensile strengths (direct tension test) were measured from $\varnothing 80 \cdot 210$ mm cylinders (first phase) and $\varnothing 150 \cdot 300$ mm cylinders (second phase). With the HSC series, standard tests on 150 mm ($\varnothing$) $\cdot$ 300 mm concrete cylinders were conducted to measure the compressive strength. Table 2 reports the main values of cylinder compressive and tensile strengths for the 14 materials tested.

In addition, among many standards available for the material characterization [28], all SFRC were characterized according to the European Standard EN 14651 [29], which requires that bending tests (3PBT) be performed on small notched beams (150 $\cdot$ 150 $\cdot$ 550 mm). Based on experimental curves concerning the total nominal stress vs. crack mouth opening displacement (CMOD), parameters $f_{R,j}$ (evaluated at four different CMOD values, i.e. 0.5, 1.5, 2.5 and 3.5 mm), and the flexural tensile strength (limit of proportionality) f_L were calculated, as listed in Table 5 (mean values).

2.3. Set-up and instrumentation

In the first phase, tensile tests (both, NSC and HSC series) were performed by means of hydraulic servo-controlled (closed-loop) testing machines. Tests were carried out under stroke control (by clamping both the rebar ends) by monitoring the specimen behavior up to the onset of the rebar strain-hardening. The deformation rate was varied from 0.1 to 0.2 mm/min up to the yield limit of the rebar. Beyond this point, the rate was progressively increased from 0.5 mm/min up to 1 mm/min, the latter at an average strain of approximately 2%.

A typical instrumented specimen of the first phase is shown in Fig. 2a: four Linear Variable Differential Transformers (LVDTs, one for each side), were employed to measure the deformation of the specimen over a length ranging from 900 mm to 950 mm (refer to the schematic drawing of Fig. 2b).

Regarding NSC elements, all RC specimens and those belonging to SFRC series 1M† were stored in a fog room (R.H. > 95%; $T = 20 \pm 2$ °C) until 2 or 3 days before testing; then they were air dried in the laboratory. All the other specimens were moist cured with wet burlap under plastic sheet until 2 or 3 days before testing, since it was not possible, for space restriction, using the same fog room. For the latter specimens, shrinkage effects were not likely totally controlled. Note that shrinkage does not significantly influence the final crack pattern and crack spacing, core of the present

Table 1
Properties of steel reinforcing bars.

	Rebar	A_s (mm^2)	d_b (mm)	E_s (GPa)	f_y (MPa)	ε_{sh} ($\times 10^{-3}$)	f_{ult} (MPa)	ε_{ult} ($\times 10^{-3}$)
Rebars used in NSC specimens	$\varnothing 10$	78	10	198	522	29.7	624	NA
	$\varnothing 20$	314	20	198	515	20.2	605	NA
	$\varnothing 30$-1†	707	30	187	554	15.8	672	NA
	$\varnothing 30$-2†	707	30	182	484	17.9	604	NA
Rebars used in HSC specimens	10M	100	11.3	199	442	27.0	564	164.0
	20M−1†	300	19.5	194	456	21.2	592	144.2
	20M−2†	300	19.5	188	525	17.3	653	111.6
	30M	700	29.9	187	376	11.0	558	177.0

† The 20M and $\varnothing 30$ bars came from two different production heats. NA is not available.

Table 2
Mechanical properties of concrete, fiber contents and free shrinkage strain measurements.

		Batch ID	f_{cm} (MPa)	f_{ctm} (MPa)	Volume fraction of steel fibers V_f						$\varepsilon_{c,shr} \times 10^{-6}$ (–)
					Fibers 30/0.62 (%)$_{vol.}$	Fibers 13/0.20 (%)$_{vol.}$	Fibers 30/0.38 (%)$_{vol.}$	Fibers 30/0.55 (%)$_{vol.}$	Fibers 50/1.05 (%)$_{vol.}$	$V_{f,tot}$ (%)$_{vol.}$	
1st Phase	NSC	0 Plain	40.5	3.71	–	–	–	–	–	–	NA
		0.5M	39.7	3.37	0.5	–	–	–	–	0.5	NA
		1M	25.4	2.60	1	–	–	–	–	1	NA
		1M†	36.4	3.50	1	–	–	–	–	1	NA
		1M+m	43.3	2.81	0.5	0.5	–	–	–	1	NA
	HSC	0 Plain	91.4	4.93	–	–	–	–	–	–	324
		FRC1	75.7	4.55	–	–	0.5	–	–	0.5	555
		FRC2	52.8	3.94	–	–	1	–	–	1	740
		FRC3	56.8	3.96	–	–	1.5	–	–	1.5	800
		FRC4	41.7	3.28	–	–	–	1.5	–	1.5	733
		FRC5	75.0	4.54	–	–	–	–	1.5	1.5	436
2nd Phase	NSC	0 Plain	47.2	3.50	–	–	–	–	–	–	0
		0.5M	40.8	3.35	0.5	–	–	–	–	0.5	0
		1M	27.4	2.85	1	–	–	–	–	1	0

† The series 1M was repeated. NA is not available.

Table 3
Characteristics of fibers employed.

Fiber ID	Type of steel	Shape	f_{uf} (MPa)	l_f (mm)	$\varnothing_f$ (mm)	$l_f/\varnothing_f$ (–)	Batch ID
30/0.62	Carbon	Hooked-end	1270	30	0.62	48.39	0.5M, 1M, 1M†, 1M+m
13/0.20	High carbon	Straight	2000	13	0.20	65.00	1M+m
30/0.38	High carbon	Hooked-end	2300	30	0.38	78.95	FRC1, FRC2, FRC3
30/0.55	Carbon	Hooked-end	1100	30	0.55	54.55	FRC4
50/1.05	Carbon	Hooked-end	1100	50	1.05	47.62	FRC5

investigation, whereas a quite high influence on the overall member response can be attributed to shrinkage. Different analytical formulation could be adopted for representing the shrinkage induced effects (i.e. Bishoff [30]), even though no corrections were done in this case (NSC samples).

With the HSC elements, free shrinkage prism tests were conducted in order to estimate the restrained shrinkage. Differently from NSC elements, in the HSRC and HSFRC specimens restrained shrinkage effects were significant since both the free shrinkage strains and reinforcement ratios were quite high. From the free shrinkage strains, the shrinkage-induced offset strain was calculated, which was necessary for the conversion of observed specimen elongations to net concrete strains [22], as further described in the paragraph "Crack formation and development".

In the second phase, the experimental program was carried out at the University of Brescia on NSC tie elements, using an available steel reacting frame conveniently adapted to the scope. Two steel plates, with bolt-holes previously machined, were welded at the ends of the specimen (see Fig. 1b) and used to connect (by pins) to the reacting rig (for details, see [24]). For further improving the test set-up, in the NSFRC 1M specimens (15 samples) the tie ends were strengthened in order to have an ultimate strengths (of the bare bar) higher than the RC/FRC tie and avoid the rebar localization at free ends. However, the choice of providing the rebar end an over-strength did not have any impact on the crack phenomenon.

Tests were carried out under stroke control and by assuming the same load-procedure previously described for the first phase. Four LVDTs, one for each side of the sample, were placed to measure the deformation of the specimen over a length of 1400 mm (members with a bar diameter of 20 and 30 mm) and 900 mm (bar diameter of 10 mm). All specimens were stored in a fog room (R.H. > 95%; T = 20 ± 2 °C) until 2 or 3 days before testing; then they were air dried in the laboratory. In the fog room, shrinkage strains were measured by means of free shrinkage prisms. Since the

measured strains were negligible, no-shrinkage offset strains were applied in the analysis of tensile members tested in the second phase.

All available values of free shrinkage strains $\varepsilon_{c,shr}$ (the mean value for each of the 14 materials) are reported in Table 2.

3. Results and discussion

3.1. Typical tensile tie behavior

The diagrams reported in Fig. 3a and in Fig. 3b provide typical responses in terms of axial load vs. average tensile member strain of fibrous and non-fibrous specimens for NSC and HSC series, respectively. The average member strain was calculated as the mean elongation of the four LVDTs, divided by the length of the base measurement. In the elastic phase, the four LVDT measurements differed of 20%, at most. During the crack formation stage, the differences in the four measurements were obviously higher, up to 60% between the two faces. After the stabilized cracking stage, the difference dropped down again at values similar to those reported in the elastic phase.

In both the diagrams (Fig. 3a and b), a comparison between one typical RC and corresponding SFRC member is provided. In addition, the response of the corresponding bare bar is reported.

The results are plotted up to a maximum average strain of 5×10^{-3} in order to properly describe the tensile behavior at SLS, where the crack and deformation control is of main importance, and also in order to assess the behavior at yielding.

In RC specimens, the elastic stiffness remained relatively high until the initial crack occurred, after which the tension stiffening behavior initiated and the overall stiffness reduced significantly. Since no fibers were included, the transmission of any residual stress across cracks was very limited, and, therefore, the load-deformation response quickly approached that of the bare bar

Table 4
Experimental program and specimen notation.

Phase	Rebar	Batch ID	b (mm)	Length, L (mm)	Reinf. ratio (%)	Clean cover (mm)	Specimen ID	s_{rm} (mm)	w_{max} (mm)
1st Phase	NSC	∅10	0 Plain					N 50/10 – 0	120	NA
			0.5M					N 50/10 – 0.5M	59	NA
			1M	50	950	3.26	20	N 50/10 – 1M	55	NA
			1M†					N 50/10 – 1M†	61	NA
			1M+m					N 50/10 – 1M+m	50	NA
		∅10	0 Plain					N 80/10 – 0	150	NA
			0.5M					N 80/10 – 0.5M	109	NA
			1M	80	950	1.25	35	N 80/10 – 1M	91	NA
			1M†					N 80/10 – 1M†	94	NA
			1M+m					N 80/10 – 1M+m	96	NA
		∅20	0 Plain					N 100/20 – 0	147	NA
			0.5M					N 100/20 – 0.5M	112	NA
			1M	100	950	3.24	40	N 100/20 – 1M	79	NA
			1M†					N 100/20 – 1M†	113	NA
			1M+m					N 100/20 – 1M+m	87	NA
		∅20	0 Plain					N 150/20 – 0	213	NA
			0.5M					N 150/20 – 0.5M	105	NA
			1M	150	950	1.42	65	N 150/20 – 1M	107	NA
			1M†					N 150/20 – 1M†	160	NA
			1M + m					N 150/20 – 1M+m	135	NA
		∅30	0 Plain	150	950	3.24	60	N 150/30 – 0	212	NA
		∅30	0 Plain	200	950	1.80	85	N 200/30 – 0	278	NA
		M10	0 Plain					H 50/10 – 0	49	0.17
			FRC1					H 50/10 – FRC1	40	0.18
	HSC		FRC2	50	1000	4.17	19.35	H 50/10 – FRC2	39	0.35
			FRC3					H 50/10 – FRC3	36	0.26
		M10	0 Plain					H 80/10 – 0	98	0.40
			FRC1					H 80/10 – FRC1	47	0.21
			FRC2	80	1000	1.59	34.35	H 80/10 – FRC2	45	0.27
			FRC3					H 80/10 – FRC3	40	0.22
		M20	0 Plain					H 100/20 – 0	101	0.45
			FRC1					H 100/20 – FRC1	53	0.25
			FRC2	100	1000	3.09	40.25	H 100/20 – FRC2	34	0.33
			FRC3					H 100/20 – FRC3	42	0.57
		M20	0 Plain					H 150/20 – 0	130	0.59
			FRC1					H 150/20 – FRC1	60	0.38
			FRC2	150	1000	1.35	65.25	H 150/20 – FRC2	62	0.26
			FRC3					H 150/20 – FRC3	57	0.58
			FRC4					H 150/20 – FRC4	82	0.36
			FRC5					H 150/20 – FRC5	69	0.44
		M30	0 Plain					H 150/30 – 0	133	0.44
			FRC1					H 150/30 – FRC1	66	0.45
			FRC2	150	1000	3.21	60.05	H 150/30 – FRC2	49	0.28
			FRC3					H 150/30 – FRC3	56	0.28
			FRC4					H 150/30 – FRC4	61	0.31
			FRC5					H 150/30 – FRC5	68	0.25
		M30	0 Plain					H 200/30 – 0	151	0.58
			FRC1					H 200/30 – FRC1	74	0.61
			FRC2	200	1000	1.78	85.05	H 200/30 – FRC2	58	0.39
			FRC3					H 200/30 – FRC3	58	0.38
			FRC4					H 200/30 – FRC4	88	0.27
			FRC5					H 200/30 – FRC5	80	0.43
2nd Phase	NSC	∅10	0					N 80/10 – 0	144	NA
			0.5%	80	1000	1.25	35	N 80/10 – 0.5M	105	NA
			1.0%					N 80/10 – 1M	102	NA
		∅20	0					N 120/20 – 0	170	NA
			0.5%	120	1500	2.23	50	N 120/20 – 0.5M	151	NA
			1.0%					N 120/20 – 1M	127	NA
		∅20	0					N 180/20 – 0	358	NA
			0.5%	180	1500	0.98	80	N 180/20 – 0.5M	234	NA
			1.0%					N 180/20 – 1M	223	NA
		∅30	0					N 180/30 – 0	232	NA
			0.5%	180	1500	2.23	75	N 180/30 – 0.5M	198	NA
			1.0%					N 180/30 – 1M	145	NA
		∅30	0					N 200/30 – 0	310	NA
			0.5%	200	1500	1.80	85	N 200/30 – 0.5M	220	NA
			1.0%					N 200/30 – 1M	197	NA

† The series 1M was repeated. NA is not available.

and the maximum load was limited by the yield strength of the rebar.

In a typical SFRC specimen, the uncracked response was similar to that of a non-fibrous specimen, as expected. After cracking, fibers provided a noticeable enhancement of the concrete toughness, ensuring a considerable residual strength through cracks (this phenomenon is defined as tension softening or hardening). Accordingly, by referring to a certain average member strain, the improved toughness due to fibers determined an increment of the average tensile strength of the undamaged concrete between

Table 5
Fracture parameters of the SFRCs according to EN 14651.

		Batch ID	Fracture parameters of the SFRCs according to EN-14651				
			f_{Lm} (MPa)	$f_{R,1m}$ (MPa)	$f_{R,2m}$ (MPa)	$f_{R,3m}$ (MPa)	$f_{R,4m}$ (MPa)
1st Phase	NSC	0.5M	5.46	5.00	4.55	4.05	3.46
		1M	4.91	5.79	5.15	4.40	3.75
		1M†	4.81	5.09	4.12	3.42	3.01
		1M+m	5.97	6.30	5.35	4.35	3.54
	HSC	FRC1	6.11	8.98	7.82	6.74	5.54
		FRC2	4.94	10.08	9.53	8.79	7.51
		FRC3	4.98	7.38	7.32	6.60	5.50
		FRC4	4.63	6.71	5.6	4.24	3.75
		FRC5	5.23	7.66	6.91	6.03	4.79
2nd Phase	NSC	0.5M	4.60	4.12	4.07	3.35	2.69
		1M	4.64	5.43	4.89	4.36	3.86

† The series 1M was repeated.
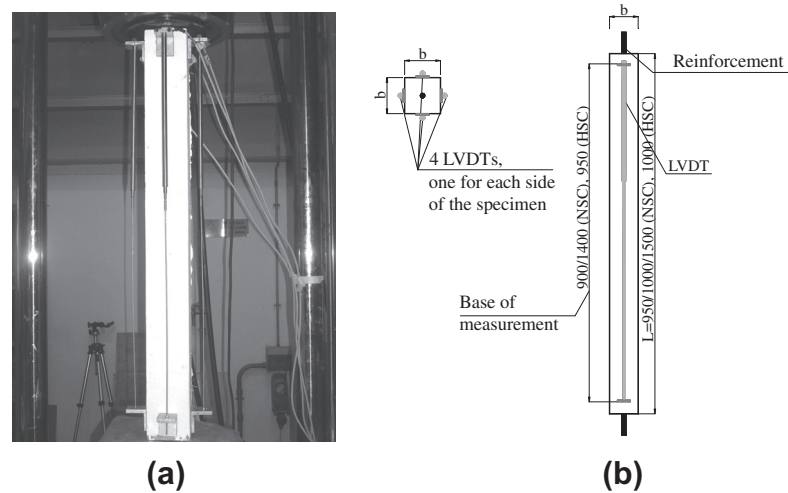
Fig. 2. Typical configuration of the tensile tie during test (a) and instrumentation (b).
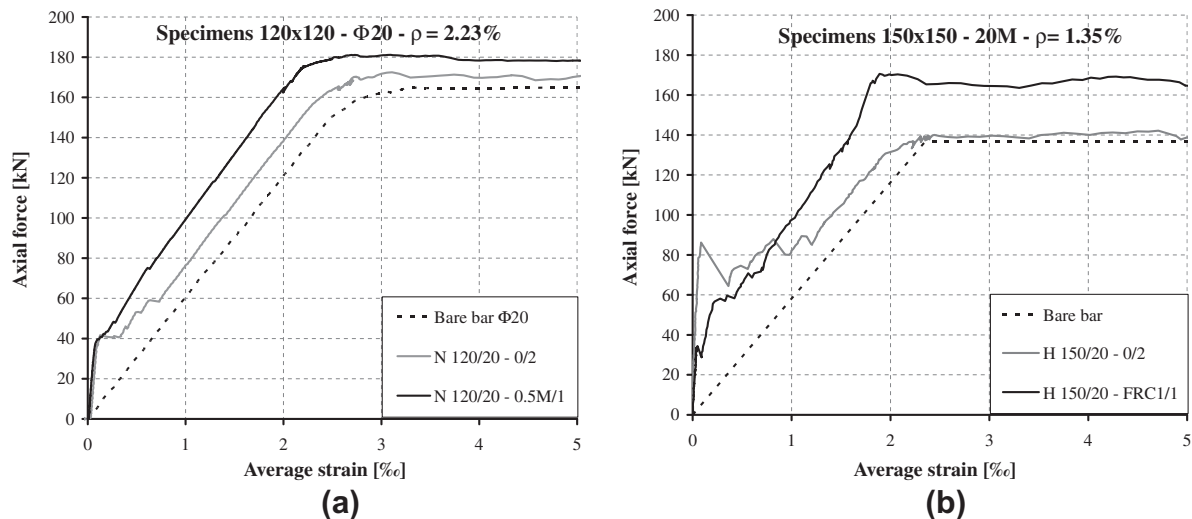
Fig. 3. Typical response of a NSRC and NSFRC (a) and HSRC and HSFRC tie elements (b).

two consecutive cracks. As a result, in both NSC and HSC tie elements, the tension-stiffening behavior of SFRC series was more pronounced than that of corresponding RC specimens. In addition, after first cracking, the reduction in load-carrying capacity was significantly more gradual in SFRC members than in RC specimens.

The improvement of the tension-stiffening can be clearly evidenced in the stabilized cracking stage for NSFRC elements (Fig. 3a) whereas it is relevant, in the HSC ties, only for average strains greater than 1×10^{-3} (Fig. 3b). The main reason is that HSFRC elements plotted in Fig. 3b experienced particularly large

shrinkage strains. This caused the apparent cracking load to decrease with respect to that of a non-fibrous concrete specimen, which, on the contrary, exhibited lower shrinkage [22].

By analyzing the typical responses of fibrous tie elements (Fig. 3a and b), the fiber resistant contribution (post-cracking strength) can be clearly shown at yielding since SFRC toughness allows the transfer of residual tensile stresses at crack with a consequent increase of the load capacity, whereas in the RC control samples this further contribution cannot be observed.

It is worthwhile mentioning that some splitting cracks were detected in both RC and SFRC specimens. For NSC series, no significant splitting cracks appeared in the members, also in the post-yielding branch, except for the RC samples having the largest rebar diameter ($\varnothing = 30$ mm) and for specimens having $\varnothing = 20$ mm and size of 100 mm. For these samples, splitting cracks appeared at a load level of around 0.8 F_{yield} (where F_{yield} corresponds to the rebar yielding).

Regarding HSC tensile ties, some splitting cracks were detected; however, these were determined to have little effect on the tensile behavior of the specimens [22].

3.2. Crack formation and development

A significant aspect of the investigation herein concerns the crack pattern and its evolution in terms of mean crack spacing. The mean crack spacing of a single specimen was evaluated by measuring the distance between visible cracks on the surface. Furthermore, the mean crack spacing of each set of samples (s_{rm}) was calculated as the mean value of the measured mean values of each single specimen. Table 4 reports all values of s_{rm} and the maximum crack width, where available.

In Fig. 4a and b, the evolution of the mean crack spacing s_{rm} is plotted as a function of the average strain up to the end of the crack formation stage for specimens N 200/30 and H 200/30, respectively. Differently from Fig. 3b, note that in HSC specimens the effect of shrinkage was computed and the cracking behavior is plotted with respect to their net concrete strains (i.e. due to stress only), according to [22]. The diagrams are plotted for the different SFRC specimens under investigation in order to evidence the influence of fiber content on the cracking behavior. With this purpose, for HSC tie elements (Fig. 4b), the curves are referred to series FRC1, FRC2, FRC3 (with fibers 30/0.38 and V_f of 0.5%, 1%, 1.5%, respectively, see Table 2). On the other hand, the NSC series (Fig. 4a) are plotted for macrofiber (30/0.62) with two dosages:

$V_f = 0.5\%$ and 1% (specimens tested in the second phase). The responses of control RC series are also plotted as a reference.

Comparing responses at a common member average strain, one can see that as the fiber content increases, the mean crack spacing decreases; this tendency is consistent for a given average strain and it also applies, as expected, at the end of the crack formation stage (i.e., onset of the stabilized cracking stage), as is well depicted in the two graphs by the horizontal asymptotes, corresponding to the final mean crack spacing. In fact, the residual post-cracking strength provided by steel fibers (at any crack) contributes to the reduction of the transmission length necessary to transfer tensile stresses in concrete through bond; hence, the mean crack spacing and the corresponding mean crack width will diminish.

The analysis of the evolution of the mean crack spacing with respect to the average member strain (for all the series investigated) demonstrates that the crack formation stage of NSRC and NSFRC specimens corresponds approximately to a range of strains varying from 0.5×10^{-3} to 1.5×10^{-3}; a similar tendency can be seen with the HSC tie elements even though the range of strain is slightly higher. In particular, according to the enhanced fiber resistant contribution, one would expect a lower value of the average strain corresponding to the end of the crack formation stage. However, a clear tendency was not observed.

Note that the comparison of SFRC series depends not only on the concrete strength but also on the fiber toughness. In particular, the NSC specimens contain fibers 30/0.62 whereas HSC samples fibers 30/0.38 (see Table 5 for details).

The diagrams plotted in Fig. 4a and b clearly confirm that, referring to the same reinforcement ratio (conventional rebar) and the same clear cover, HSRC elements exhibit smaller mean crack spacings and consequently smaller crack widths, relative to corresponding NSRC members. This tendency is consistent for average member strains ranging from the crack formation stage to the stabilized cracking stage. The same trend can be also outlined for SFRC specimens, even though the rate of reduction of crack spacing should not be attributed only to concrete strength but also to the SFRC toughness, as aforementioned.

Referring to the member average strain at the end of the crack formation stage, no significant effects of the concrete strength on this parameter was observed.

In Fig. 5 the mean crack spacing s_{rm} is plotted vs. the key parameter $\varnothing/\rho_{eff}$, which is generally included in many building codes for the prediction of the mean crack spacing. In particular, in Fig. 5a the experimental results are plotted for RC members, whereas in
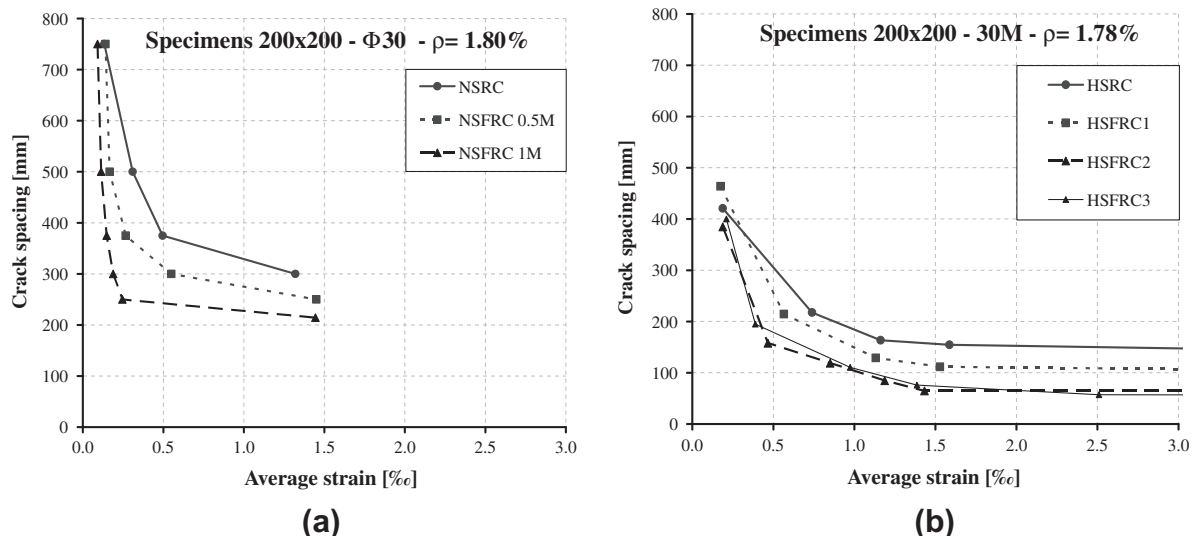

Fig. 4. Evolution of the mean crack spacing of SFRC and RC series: NSC (a), HSC (b).

Fig. 5b the trend of SFRC members with a total $V_f \leqslant 1\%$ is reported (the results include macrofibers, macro + microfibers according to all combinations presented in Table 4). In the two plots, note that NSC corresponds to tie elements having a cylinder concrete compressive strength lower than 50 MPa, whereas HSC refers to members with a higher value. The trend reported for RC elements confirms the tendency previously observed in Fig. 4a and b: by referring to specimens having the same $\varnothing/\rho_{eff}$, the use of HSC results in a considerable reduction of s_{rm}, with percentages up to 45%. Since several formulations proposed in the literature or in design codes define the crack spacing to be linearly proportional to the parameter $\varnothing/\rho_{eff}$, it is meaningful to evaluate the dispersion of results according to a linear regression. As depicted in Fig. 5a, the coefficient of correlation R^2 is equal to 0.92 for the NSRC samples and 0.83 for HSRC elements. Basically, a possible linear relationship between s_{rm} and $\varnothing/\rho_{eff}$ could be reliable, even though that should be probably a function of the concrete strength, differently from most of published relationships of s_{rm}.

The s_{rm} vs. $\varnothing/\rho_{eff}$ trend for SFRC ties with $V_f \leqslant 1\%$, as depicted in Fig. 5b, is rather similar: a global reduction of the mean crack spacing with higher concrete strength is noticeable. Furthermore, as expected, the crack spacing of the SFRC series are smaller than the corresponding RC due to the enhanced material toughness. The linear coefficient of correlation R^2 ranges within 0.64–0.68, indicating a poorer fitting. The reduction of the R^2 coefficient, with respect to control RC samples, is probably due to the higher dispersion of results in presence of fibers: in fact, for the sake of simplicity, different combinations of fiber reinforcement (belonging to diverse toughness ranges) are included in the comparison shown in Fig. 5b. In other words, both the effect of concrete strength and concrete toughness is included in this graph.

In order to better capture the experimental trends previously described, the mean crack spacing s_{rm} was plotted with respect to the concrete compressive strength (f_c), in Fig. 6a and b, for four selected ranges of $\varnothing/\rho_{eff}$, respectively for RC and SFRC series.

The diagrams plotted in Fig. 6a for RC series further confirm that, for a given range of $\varnothing/\rho_{eff}$, the increase in compressive strength is non-linearly related with a reduction of the crack spacing, as well depicted by the regression dashed curves superimposed on the diagrams (regression based on a polynomial function). The same trend was observed for all SFRC series (Fig. 6b) even though the greater dispersion of SFRC fracture properties make apparently this phenomenon less evident. In fact, the obtained polynomial regression curves tend to be much closer one to the other, owing to the considerable experimental scatter.

However, a broader test database on SFRC is necessary to clearly identify the effect of each parameter on the crack spacing.

3.3. Discussion of crack spacing formulations

A number of crack spacing formulations for RC members (without fibers) can be found in literature and in building codes. In this section the following formulations will be considered and compared against the experimental results:

– MC 1978 [25].
– MC 2010 [1].

Referring to non-fibrous members, plots of the mean crack spacing predicted by MC 1978 and MC 2010 against those observed from experiments are presented in Fig. 7a and b, respectively. In the case of NSRC specimens, a quite good agreement can be seen with experimental data (mean percentage error – MPE, around 24% for both formulations). On the other hand, it is evident that neither model adequately predicts the crack spacing of HSRC (MPE: 92% for MC 1978 and 84% for MC2010) since, as already mentioned, both approaches do not include the effect of the concrete compressive strength.

The relationship proposed by MC 2010 [1], which applies also to structures reinforced by a combination of fibers and conventional rebars, takes into account the fiber resistant contribution by means of a reduction of the introduction length ($l_{s,max}$, generally assumed for RC elements) with f_{Ftsm}, factor that includes the FRC toughness ($f_{Ftsm} = 0.45 \, f_{R,1m}$). The starting point of the MC 2010 approach is the introduction of the design crack width (w_d) which corresponds to the maximum crack width (w_{max}) defined as follows:

$$w_d = w_{max} = 2 \cdot \varepsilon_{sm} \cdot l_{s,max}. \tag{1}$$

Assuming that:

$$w_d = w_k = 1.7 \cdot w_m = 1.7 \cdot \varepsilon_{sm} \cdot s_{rm}. \tag{2}$$

The following expression can be derived:

$$s_{rm} = 1.17 \cdot l_{s,max} = 1.17 \cdot \left[k \cdot c + \frac{1}{4} \cdot \frac{\phi}{\rho_{eff}} \cdot \frac{(f_{ctm} - f_{Ftsm})}{\tau_{bm}} \right]$$
$$= 1.17 \cdot \left[k \cdot c + \frac{1}{4} \cdot \frac{\phi}{\rho_{eff}} \cdot \frac{(f_{ctm} - 0.45 \cdot f_{R,1m})}{\tau_{bm}} \right]. \tag{3}$$
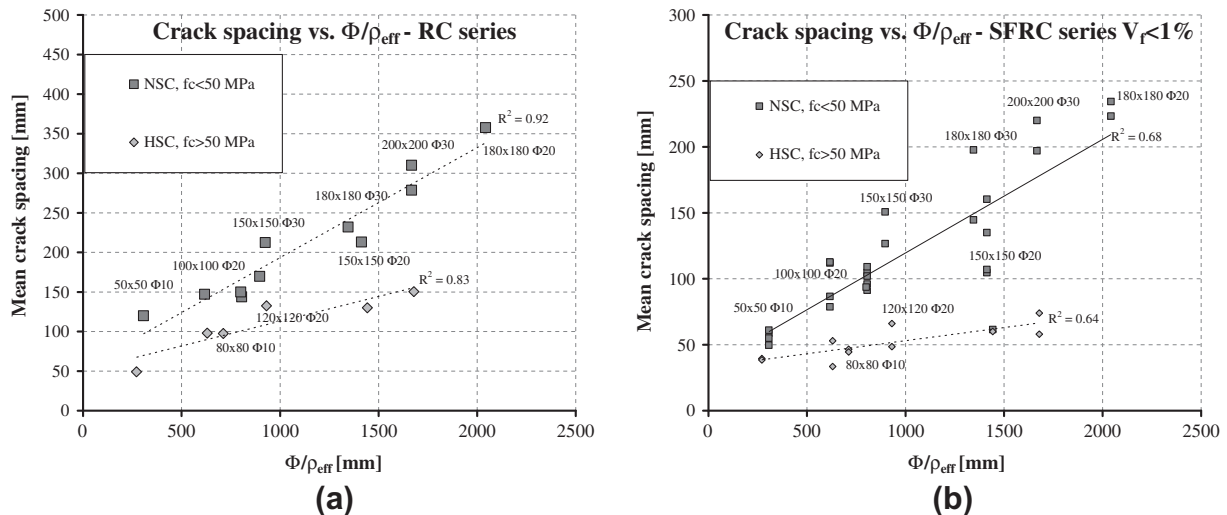

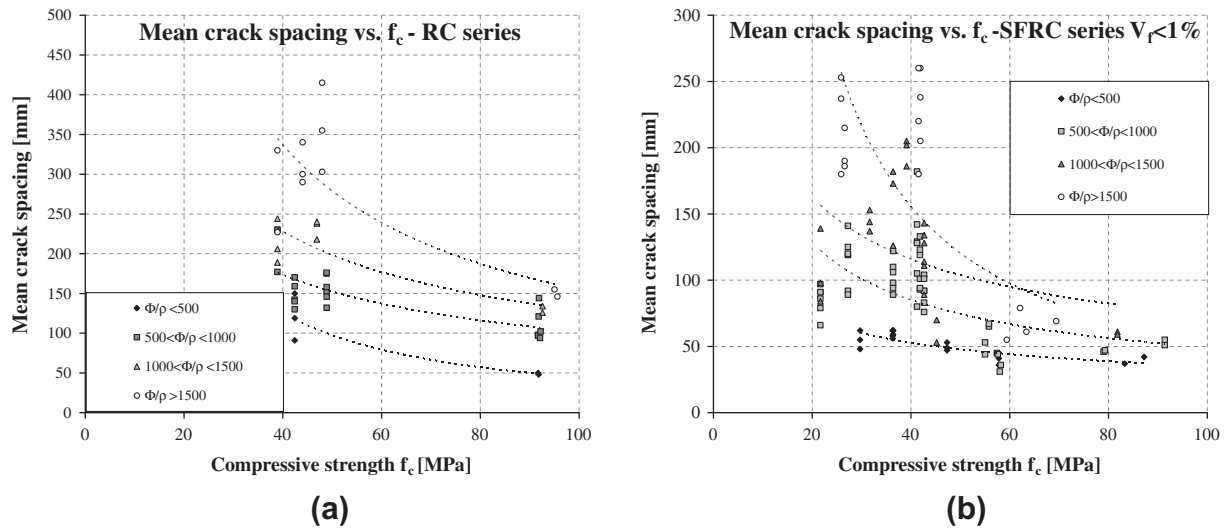**Fig. 5.** Crack spacing vs. $\varnothing/\rho_{eff}$: RC series (a) SFRC series (b).

Fig. 6. Mean crack spacing vs. concrete compressive strength f_c: RC series (a) SFRC series (b).
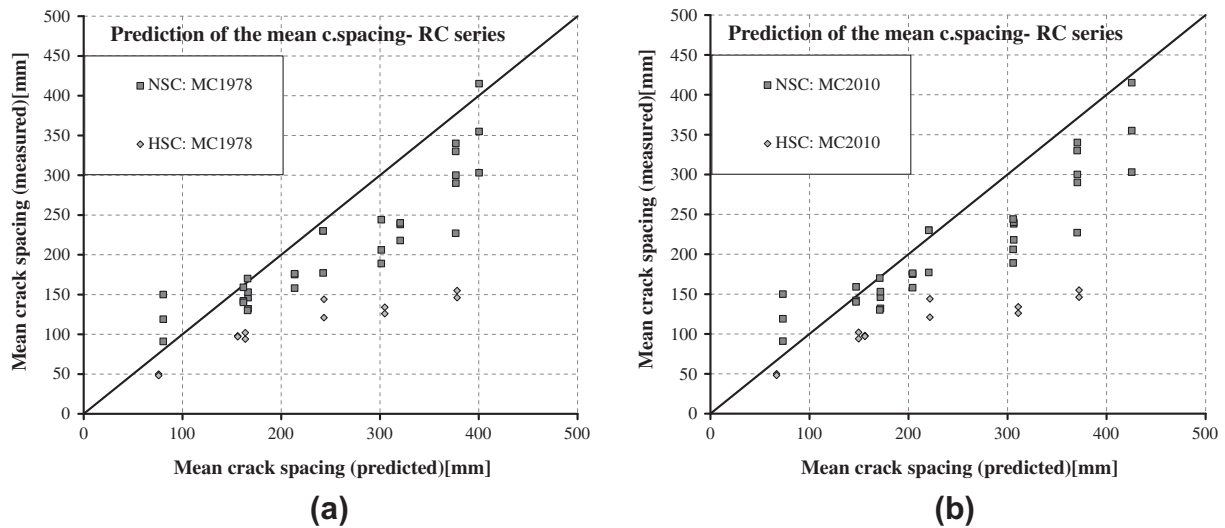

Fig. 7. Crack spacing prediction for RC series: MC1978 (a), MC2010 (b).

Eq. (3) has been applied based on the fracture parameters (mean values) reported in Table 5. Moreover, according to MC 2010, the factor k was assumed equal to 1 while the bond stress (τ_{bm}) over the concrete tensile strength (f_{ctm}) ratio was assumed equal to 1.8 [19], even for SFRC specimens (there is no evidence up to now about a possible change in the τ_{bm}/f_{ctm} in FRC elements). The comparison between Eq. (3) and the experimental results are presented in Fig. 8. Regarding NSFRC series, quite good agreement with test results emerges (MPE = 32%), even though in the 18% of the entire set of samples (all belonging to 1st phase, series 1M, 1M+m and FRC2; see Table 2) the term in the round brackets (Eq. (3)) does not have any physical meaning as it results negative and s_{rm} is only balanced by the effect of the concrete cover $k \cdot c$. For HSFRC series MPE = 54%. If at first glance it is surprising noticing that the MPE is lower in the HSFRC series than in the corresponding HSRC series, a more detailed evaluation suggests that this trend is, once again, likely due to a fortunate combination of concrete cover and fiber contribution, in which one factor balances the other.
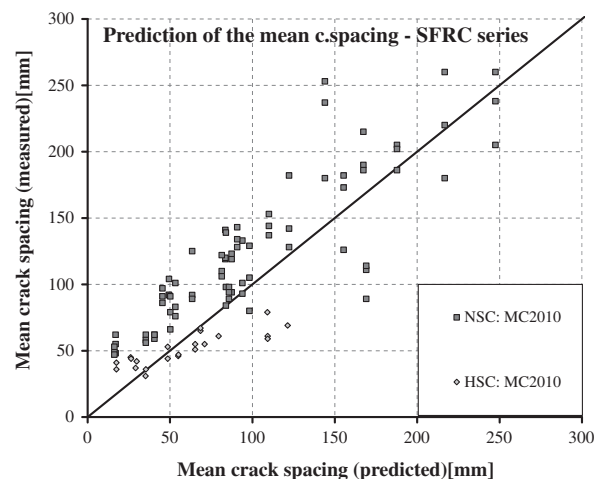

Fig. 8. Crack spacing prediction for SFRC series, MC2010.

4. Conclusions

In the present paper, a broad experimental study within a joint research program between the Universities of Brescia (Italy) and Toronto (Canada) is presented, aiming at evaluating the cracking behavior of RC and SFRC ties, with special focus on the effect of concrete compressive strength. A series of 109 NSC tie tests have been carried out in Brescia while Toronto tested a series of 59 members made of HSC.

Based on the results and on the discussion presented, the following main conclusions might be drawn:

– The use of HSC results in a noticeable reduction of the mean crack spacing with respect to NSC. This tendency was clearly evidenced for both RC and SFRC specimens: a reduction of around 40% can be reported with increasing strength in non-fibrous elements and a decrease, up to 50%, in SFRC specimens.
– The stabilized cracking stage does not seem to be influenced either by the enhanced toughness (in SFRC materials) or concrete grade: in both the cases, a higher number of cracks form, without a clear indication that the stabilized cracking stage develops later or earlier than in both NSRC or NSFRC elements.
– SFRC influences the behavior of tension-ties at SLS, by reducing crack width and resulting in crack patterns with narrower and closely spaced cracks.
– SFRC stiffens the post-cracking response of RC members and it is effective in diminishing the deflections of the structures (this is a key-point for SLS design).
– The currently available crack spacing models herein investigated (MC 1978 and MC 2010) for traditional RC are not adequate for predicting s_{rm} in HSC members since results markedly depend on the concrete compressive strength, which is not taken into account in any code predictions. Therefore, improved formulations are strongly required in order to include the effect of f_c both in SFRC and RC elements.
– The MC 2010 model for predicting s_{rm} in SFRC elements generally predicts with sufficient accuracy the experimentally observed data on NSC series.
– Improved formulations are strongly required in order to include the effect of compressive strength both in fibrous and non-fibrous elements.

Further studies have to be planned and performed for better understanding the relationship between SFRC toughness and reinforcement ratio and for improving analytical models in order to better predict the average crack spacing.

Acknowledgments

References

[1] Model Code 2010, Final Complete Draft, Fib Bull: 2012 [65 and 66, March 2012-ISBN 978-2-88394-105-2 and April 2012-ISBN 978-2-88394-106-9].

[2] ACI Committee 544. Design considerations for steel fibre reinforced concrete, ACI 544.4R-88. ACI Farmington Hills (MI): American Concrete Institute; 1999.

[3] Di Prisco M, Felicetti R, Plizzari GA, editors. Fiber-reinforced concrete. BEFIB 2004. Bagneux (France): RILEM Publications SARL, PRO39; 2004.

[4] Gettu R, editor. Fibre reinforced concrete: design and applications. BEFIB 2008. Bagneux (France): RILEM Publications SARL, PRO60; 2008.

[5] Barros JAO, et al. editors, Fibre reinforced Concrete: challenges and opportunities, In: CD and proceeding book of abstracts of the eighth RILEM international symposium (BEFIB 2012) Guimarães (Portugal), September 19–21; 2012, [ISBN: 978-2-35158-132-2; e-ISBN: 978-2-35158-133-9, 2012].

[6] di Prisco M, Plizzari GA, Vandewalle L. Fibre reinforced concrete: new design perspectives. Mater Struct 2009;42(9):1261–81.

[7] Plizzari GA, Tiberti G. Structural behaviour of SFRC tunnel segments, In: Proceedings of the 6th international conference on fracture mechanics of concrete and concrete structures (FraMCos 2007), vol. 3, Carpinteri A, Gambarova P, Ferro G, Plizzari GA. editors, Catania (Italy), June 17–22; 2007. p. 1577–1584. [ISBN 978-0-415-44066-0].

[8] Minelli F, Plizzari GA. On the effectiveness of steel fibers as shear reinforcement. ACI Struct J 2013;110(3):379–89 [ISSN 0889-3241].

[9] Conforti A, Minelli F, Plizzari G. Wide-shallow beams with and without steel fibres: a peculiar behaviour in shear and flexure. Compos Part B: Eng 2013;51:282–90. http://dx.doi.org/10.1016/j.compositesb.2013.03.033 [ISSN 1359-8368].

[10] Meda A, Minelli F, Plizzari GA. Flexural behaviour of RC beams in fibre reinforced concrete. Compos Part B: Eng 2012;43(8):2930–7. http://dx.doi.org/10.1016/j.compositesb.2012.06.003 [ISSN 1359-8368].

[11] Beeby AW. The prediction of cracking in reinforced concrete members, PhD thesis, University of London; 1971.

[12] Beeby AW, Scott RH. Cracking and deformation of axially reinforced members subjected to pure tension. Mag Concr Res 2005;57(10):611–21.

[13] A Borosnyói, GL Balázs. Models for flexural cracking in concrete: the state of the art. Structural Concrete 2005;6(2):53–62 [ISSN: 1464-4177, E-ISSN 1751-7648].

[14] Mitchell D, Abrishami HH. Influence of steel fibres on tension stiffening. ACI Struct J 1996;94(6):769–76.

[15] Fields K, Bischoff PH. Tension stiffening and cracking of high strength reinforced concrete tension members. ACI Struct J 2004;101(4):447–56.

[16] Bischoff PH. Tension stiffening and cracking of steel fibre reinforced concrete. J Mater Civil Eng 2003;15(2):174–82.

[17] Noghabai K. Effect of tension softening on the performance of concrete structures. Experimental, analytical and computational studies, Doctoral thesis, Division of Structural Engineering, Lulea University of Technology; 1998. p. 186.

[18] Chiaia B, Fantilli AP, Vallini P. Evaluation of crack width in FRC structures and application to tunnel linings. Mater Struct 2009;42:339–51. http://dx.doi.org/10.1617/s11527-008-9385-7 [ISSN: 1359-5997].

[19] Leutbecher T, Fehling E. Tensile behavior of ultra-high performance concrete reinforced with reinforcing bars and fibers: minimizing fiber content. ACI Struct J 2012;109(2):253–64.

[20] Tiberti G, Plizzari G, Blom C.B.M, Walraven J. Concrete tunnel segments with combined traditional and fiber reinforcement, In: International fib symposium tailor made concrete structures, 2008. May 19–22, 2008, Amsterdam, The Netherlands, pp. 199–205, Taylor & Francis Group (CRC Press), ISBN: 9780415475358, DOI: 10.1201/9781439828410.ch37.

[21] Reza Esfahani M, Rangan BV. Local bond strength of reinforcing bars in normal strength and high-strength concrete (HSC). ACI Struct J 1998;95(2):96–106.

[22] Deluce JR, Vecchio FJ. Cracking behavior of steel fiber-reinforced concrete members containing conventional reinforcement. ACI Struct J 2013;110(3):481–90.

[23] Minelli F, Tiberti G, Plizzari GA. Crack control in RC elements with fibre reinforcement, ACI Special Publication ACI SP-280: Advances in FRC durability and field applications CD-ROM, Vol. 280, Editors: Corina-Maria Aldea, Mahmut Ekenel, December 2011. p. 76-93 [ISSN: 01932527 ISBN: 978161839797-3] .

[24] Tiberti G, Minelli F, Plizzari GA. Crack control in fibrous RC Elements, In: Proceedings of the eighth RILEM international symposium (BEFIB 2012) fibre reinforced concrete: challenges and opportunities, J.A.O Barros et al., editor, September 19–21; 2012., extended abstract on p. 187-188, ISBN: 9782351581322; full paper on CD, p. 12, e-ISBN: 9782351581339.

[25] CEB–FIP model code for concrete structures, Comité Euro-International du Béton and Fédération Internationale de la Précontrainte. 3rd ed., CEB, Paris, France; 1978.

[26] UNI EN10080, Steel for the reinforcement of concrete – weldable reinforcing steel; 2005. p. 25.

[27] CSA G30.18-09, Carbon steel bars for concrete reinforcement; 2009. p. 32.

[28] Minelli F, Plizzari GA. A new round panel test for the characterization of fiber reinforced concrete: a broad experimental study. ASTM J Test Eval 2011;39(5):889–97. http://dx.doi.org/10.1520/JTE103392 [ISSN 1945-7553].

[29] EN 14651, Test method for metallic fibre concrete – measuring the flexural tensile strength (limit of proportionally (LOP), residual), European Committee for Standardization; 2005. pp. 18.

[30] Bischoff PH. Effect of shrinkage on tension stiffening and cracking in reinforced concrete. Can J Civil Eng 2001;28(3):363–74.